MTL TR 92-59

(2)

EVALUATION OF 8090 AND WELDALITE-049 ALUMINUM-LITHIUM ALLOYS

THOMAS M. HOLMES and ERNEST S. C. CHIN
MATERIALS PRODUCIBILITY BRANCH

PAUL J. HUANG
METALS RESEARCH BRANCH

ROBERT E. PASTERNAK
MATERIALS TESTING AND EVALUATION BRANCH

September 1992

US ARMY
LABORATORY COMMAND
MATERIALS TECHNOLOGY LABORATORY

U.S. ARMY MATERIALS TECHNOLOGY LABORATORY
Watertown, Massachusetts 02172-0001

The findings in this report are not to be construed as an official Department of the Army position, unless so designated by other authorized documents.

Mention of any trade names or manufacturers in this report shall not be construed as advertising nor as an official indorsement or approval of such products or companies by the United States Government.

DISPOSITION INSTRUCTIONS

Destroy this report when it is no longer needed.
Do not return it to the originator.

REPORT DOCUMENTATION PAGE

READ INSTRUCTIONS BEFORE COMPLETING FORM

1. REPORT NUMBER: MTL TR 92-59	2. GOVT ACCESSION NO.
3. RECIPIENT'S CATALOG NUMBER	
4. TITLE (and Subtitle): EVALUATION OF 8090 AND WELDALITE-049 ALUMINUM-LITHIUM ALLOYS	5. TYPE OF REPORT & PERIOD COVERED
6. PERFORMING ORG. REPORT NUMBER	
7. AUTHOR(s): Thomas M. Holmes, Ernest S. C. Chin, Paul J. Huang, and Robert E. Pasternak	8. CONTRACT OR GRANT NUMBER(s)
9. PERFORMING ORGANIZATION NAME AND ADDRESS: U.S. Army Materials Technology Laboratory, Watertown, Massachusetts 02172-0001, SLCMT-MEM	10. PROGRAM ELEMENT, PROJECT, TASK AREA & WORK UNIT NUMBERS
11. CONTROLLING OFFICE NAME AND ADDRESS: U.S. Army Laboratory Command, 2800 Powder Mill Road, Adelphi, Maryland 20783-1145	12. REPORT DATE: September 1992
	13. NUMBER OF PAGES: 34
14. MONITORING AGENCY NAME & ADDRESS(if different from Controlling Office)	15. SECURITY CLASS. (of this report): Unclassified
	15a. DECLASSIFICATION/DOWNGRADING SCHEDULE

16. DISTRIBUTION STATEMENT (of this Report)

Approved for public release; distribution unlimited.

17. DISTRIBUTION STATEMENT (of the abstract entered in Block 20, if different from Report)

18. SUPPLEMENTARY NOTES

19. KEY WORDS (Continue on reverse side if necessary and identify by block number)

Aluminum-lithium alloys
Mechanical properties
Microstructure
Ballistic properties
Fractography

20. ABSTRACT (Continue on reverse side if necessary and identify by block number)

(SEE REVERSE SIDE)

Block No. 20

ABSTRACT

Aluminum-lithium (Al-Li) alloys with their high strength, high stiffness, and low density continue to be of great interest to the aerospace industry. The microstructure, properties and fracture of 8090-T8771 and Weldalite™ 049-T8 Al-Li alloys were studied at MTL in participation with a cooperative round robin sponsored by the Air Force Advanced Aluminum Alloy Test Program.

Both 8090 and Weldalite Al-Li alloys demonstrate superior strength to weight ratios compared to the 2519 and 5083 aluminum armor alloys. The 8090 alloy possesses comparable mechanical and ballistic properties to 2519, while providing an 8% reduction in density. The Weldalite has a comparable density to 2519 but demonstrates improvements of over 25% in yield strength, ultimate tensile strength and fracture toughness. Both Al-Li alloys display significantly improved axial fatigue properties over 2519. Under static loading, both materials display mixed modes of transgranular shear, microductility and intersubgranular failure. Under ballistic testing, both alloys display mixed modes of dynamic failure by plugging, spalling and delamination.

Whether the goal is to reduce weight or to improve strength, Al-Li alloys offer significant potential for replacing alloys such as 2519 and 5083 as lightweight, high-strength structural armor materials.

CONTENTS

INTRODUCTION

Aluminum-lithium (Al-Li) alloys continue to be of great interest to the aerospace industry. High strength, high stiffness, and low density are some of the attractive properties found in Al-Li alloys. Weldability and ballistic protection are also crucial material properties for applications in a number of Army systems. From 1991-1992, the U.S. Army Materials Technology Laboratory (MTL) collaborated with the Air Force in their Cooperative Test Program on Advanced Aluminum Alloys. The MTL's participation included testing and evaluation of Al-Li alloys and aluminum-iron alloys. This report covers the experimental results and analysis performed on the 8090 extrusions and Weldalite™ 049 plates. The aluminum-iron study will be covered at a later date.

The principle strengthening mechanism in most Al-Li alloys is attributed to the precipitation of coherent δ' (Al_3Li) particles.[1-3] These precipitates have slip systems that are coincident with the matrix and are easily sheared by moving dislocation lines. Once sheared, the reduced flow stress allows for substantial planar slip. As dislocations pile up at the grain boundaries, the resultant stress concentrations may cause transgranular shear.[1,2] For under- and peak-aged conditions, δ (AlLi) precipitates at high angle grain boundaries at the expense of local δ'. For overaged conditions, δ also precipitates at low angle boundaries. The dissolution of δ' precipitates results in precipitate free zones (PFZ's) at the high angle boundaries. PFZ's at low angle boundaries have only been observed for Al-Li alloys with high Cu:Li ratios.[3] The absence of δ' in the PFZ's causes strain localization in the vicinity of the grain boundaries and leads to intergranular failure with some micro dimpling.[2] The presence of PFZ's at sub grain boundaries leads to reductions in ductility and fracture toughness.[1]

The detrimental effects of the δ' PFZ's can be overcome by alloy additions that lead to coprecipitation of additional phases up to the grain boundary.[4-7] Additions of copper and magnesium lead to solid solution strengthening by uniform dispersions of θ' (Al_2Cu) in underaged conditions. The δ' precipitates have also been identified to form rings around the θ' precipitates.[5] For peak aged conditions, incoherent precipitates such as S' (Al_2CuMg) and T_1 (Al_2CuLi) nucleate at subgrain boundaries and dislocations.[2] The fraction of S' and T_1 precipitates is enhanced by cold working due to the increase in dislocation density.[6,7]

EXPERIMENTAL PROCEDURES

The 8090 material obtained from the Air Force for evaluation was in the form of an "L"-shaped extrusion with a T8771 temper. Prior to receiving the material, the extrusions were each sectioned into two portions, referred to as the "bar" and "flange" in Figure 1. The flange portion had a thickness of about 0.5 inch (12.7 mm), while the bar was 1.50 inch (38.1 mm) thick. The Weldalite™ 049 plates obtained from the Air Force had a thickness of 0.50 inch (12.7 mm) and were heat treated to the T6 condition. The characterization of these materials consisted of chemical analysis, metallography, measurement of mechanical and ballistic properties, and a fractographic analysis of the failed specimens.

Analytical Methods

Chemical analysis was performed by inductively coupled argon plasma emission spectroscopy and atomic absorption spectroscopy. The densities of the Al-Li alloys were determined by the Archimedes technique. Microstructural characterization was performed through methods of optical and electron microscopy. Metallographic specimens were prepared and etched with Keller's reagent. A scanning electron microscope (SEM) equipped with energy dispersive spectroscopy (EDS) was utilized for detailed fractographic analysis.

Mechanical Characterization

Threaded round tensile specimens of 0.25 inch (6.35 mm) diameter were tested to obtain 0.2% offset yield strength, ultimate tensile strength, Young's modulus, and percent elongation. Specimens were tested on a 20 KIP electromechanical tension/compression machine with a 5,000-lb load cell at a cross-head speed of 0.02 in./min. Testing was conducted in accordance with ASTM Standard B 557-84.[8] Short transverse specimens could not be obtained for Weldalite due to thickness constraints of the plates. Short transverse specimens were prepared for the 8090 alloy utilizing subsized 0.10 inch (2.54 mm) diameter specimens machined from the bar portion of the L-shaped extrusions.

Solid cylindrical compression specimens were prepared in 0.5 inch (12.7 mm) diameters with 3:1 length:diameter ratios. Specimens were tested on a 50 KIP electromechanical tension/compression machine with a 50,000 lb load cell at a cross-head speed of 0.1 in./min. Testing was conducted in accordance with ASTM Standard E 9-89.[8] Since ductile materials generally do not display a compressive failure load, the tests were terminated after a 5% drop in load. The ultimate compressive strength was then determined from the maximum recorded load.

Shear specimens were prepared to the same configuration as the cylindrical compression specimens. Testing was conducted in accordance with ASTM Standard B 565-87.[8] The double shear configuration was utilized and the rig was operated under compression. Specimens were tested on a 50 KIP electromechanical tension/compression machine with a load cell of 50,000 lbs at a cross-head speed of 0.1 in./min.

Fracture toughness compact tension specimens were precracked and tested in accordance with ASTM Standard E 399-92.[8] The crack plane orientation code of the standard specifies the first letter of a hyphenated code as representing the direction of the tensile axis while the second letter refers to the direction of crack propagation. Specimens of 0.5 inch (12.7 mm) thickness were prepared in the L-T and T-L directions. For the 8090 alloy, 0.75 inch (19.06 mm) thick specimens were prepared in the S-L direction from the bar portion of the extrusion. Specimens were tested on a Servo-hydraulic testing machine at a cross-head speed of 0.1 in./min.

Threaded round axial fatigue specimens with 0.20 inch (5.08 mm) diameters were prepared in the longitudinal direction. Testing was conducted in accordance with ASTM Standard E 466-82.[8] The specimens were tested under ambient conditions, at a maximum/minimum stress ratio (R) of 0.1. The Weldalite specimens were tested on a Servo-hydraulic testing machine at a test frequency of 10 Hz. The 8090 specimens were tested on a Satec rotating mass testing machine at a test frequency of

30 Hz. The minor difference in test frequency falls well within the allowable range of test conditions specified by the standard.

Ballistic Testing

Determination of the V_{50} ballistic limits against 7.62 mm (.30 caliber) M2 armor piercing (AP) and 12.7 mm (.50 caliber) fragment simulating projectile (FSP) munitions was made in accordance with U. S. Army Test and Evaluation Command Test Procedure 2-2-710 DRSTE-RP-702-101. The V_{50} ballistic limit is defined as the velocity at which a specific projectile will have a 50% probability of causing perforation of a witness plate behind the test plate. Such perforations may be caused by either the projectile or by spalling of the armor target itself.

RESULTS AND DISCUSSION

Materials Characterization

1. Chemical Analysis

Table 1 summarizes the chemical analysis of 8090 and Weldalite in comparison to the 2090 Al-Li alloy.[9] Low Cu:Li and Cu:Mg ratios are observed in 8090. Aluminum-lithium alloys with low Cu:Li ratios have been shown to result in the precipitation of δ', δ and T_1.[5,10] Increasing the magnesium content lowers the Cu:Mg ratio and promotes the formation of the S' precipitates.[7] These ratios account for the formation of δ', δ , T_1 and S' in 8090, identified in the literature.[2,6,7]

The chemical analysis of Weldalite reveals high Cu:Li and Cu:Mg ratios. High Cu:Li ratios have been demonstrated to lead to the precipitation of δ', δ and θ' at peak aged conditions.[10] Weldalite has been identified as containing δ' and θ' precipitates under natural aging conditions, while T_1 is present after artificial aging.[11] The addition of silver is believed to enhance the nucleation of T_1 in Weldalite.

The 2090 alloy previously studied, contains an intermediate Cu:Li ratio and has been identified as containing fractions of T_1, δ' and θ'-like phase, possibly T_2 (Al_6CuLi_3).[12-14] Both 8090 and Weldalite alloys exhibit lower iron impurity levels than previously detected in 2090. Minor increases in the iron and silicon impurity contents can result in significant reductions in fracture toughness.[12,15]

Table 1. CHEMICAL ANALYSIS

Alloy/ (wt%)	Li	Cu	Mg	Zr	Ag	Fe	Si	Al
8090 Extrusion	2.24	1.11	0.72	0.12	-	0.044	0.058	Bal.
Weldalite Plate	1.37	4.28	0.41	0.15	0.38	0.028	0.044	Bal.
2090 Plate [9]	2.02	2.47	0.01	0.11	-	0.06	0.04	Bal.

All three Al-Li alloys utilize alloying additions of zirconium to refine the grain size by the precipitation of β' (Al_3Zr) during solutionization.[10-12,16] Dispersed β' particles provide a boundary drag pressure resisting grain growth after recrystallization.[17-19] The β' precipitates have also been identified as preferential sites for nucleation and growth of δ' because they possess the same crystal structure.[20] This leads to the frequent observance of δ' rings around β' in 8090[20,21] and 2090.[13] The θ' precipitates also form rings around β'.[5] The increase in diameter with the composite particles results in accelerated aging kinetics in these Al-Li alloys.[22]

2. Metallography

Composite micrographs of polished and etched Al-Li materials were constructed in order to show the aspect ratios of the grains with respect to the longitudinal (L), transverse (T) and short transverse (S) axes, as defined in Figure 1. The microstructures of the bar and flange portions of the 8090 extruded L-shaped bar are revealed in Figure 1-A and B, respectively. Both portions display elongation of the grains in the extrusion direction (L). Recrystallization is more pronounced in the bar portion of the extrusion. The flange portion of the 8090 extrusion has a thickness of 0.5 inch and displays an elongation of the grains in both L and T directions. This is similar to that observed in the Weldalite plate in Figure 1-C, where the longitudinal axis is defined as the rolling direction. The Weldalite plate possesses a significantly smaller grain size and a higher degree of recrystallization than observed in either portion of the 8090 extrusion.

Scanning electron micrographs of 8090 and Weldalite metallography specimens reveal the locations of coarse precipitates within the alloys. The scanning electron micrograph of 8090 under backscattered electron imaging (BEI) in Figure 2-A displays the presence of precipitates located at the boundaries of recrystallized grains. Since these precipitates appear darker in contrast than the matrix under BEI, they must be rich in an element of lower atomic weight than the aluminum. Analysis of these precipitates by EDS indicates only the presence of aluminum. The EDS system is unable to detect elements with atomic weights less than beryllium. As a result, these Al-Li precipitates identified by BEI and EDS are most likely δ (AlLi). The large fraction of Al-Li precipitates observed at the boundaries generally indicate the presence of extensive PFZ's in the alloy.[2,3]

The micrograph of Weldalite in Figure 2-B reveals the presence of strings of precipitates decorating grain and subgrain boundaries. These Al-Cu-Fe rich particles, as indicated by EDS, may be Cu_2FeAl_7 precipitates identified in the literature.[13,15] Second phase stringers of particles larger than one micron are known to act as nucleation sites for high angle subgrains.[17-18]

Static Behavior

1. Mechanical Properties

For purposes of this evaluation, the mechanical properties of the Al-Li were compared to those of 2519 and 5083 aluminum armor alloys. These results are presented below in Table 2 with respect to the specimen orientation. The data sheets for mechanical testing are presented in Appendices A (8090) and B (Weldalite). The 8090 extrusions exhibited slight improvements in ultimate tensile strength and

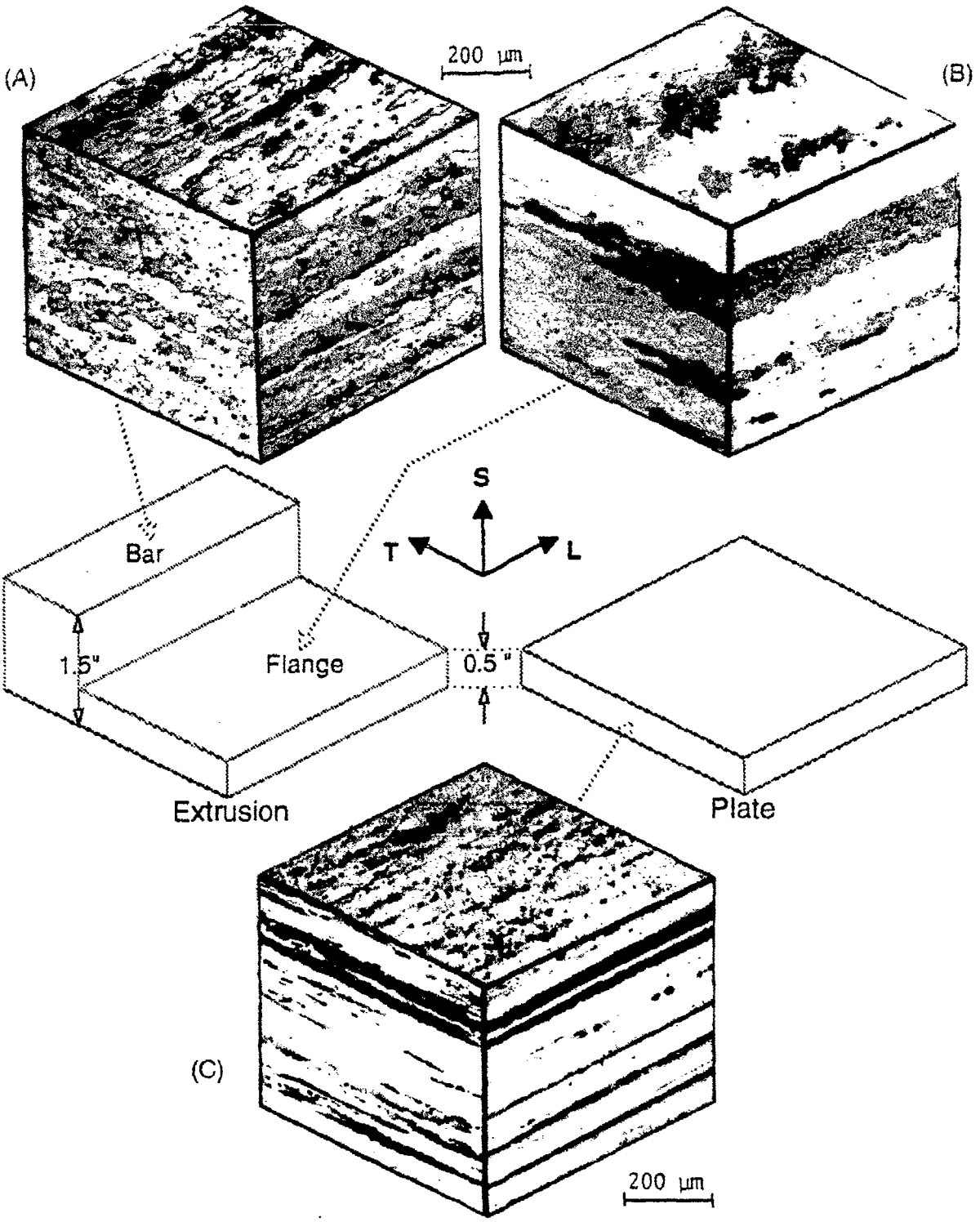

Figure 1. Composite optical micrographs revealing grain aspect ratios with respect to the extrusion or rolling direction; (A) 8090 extrusion, bar section, (B) 8090 extrusion, flange section, and (C) Weldalite plate.

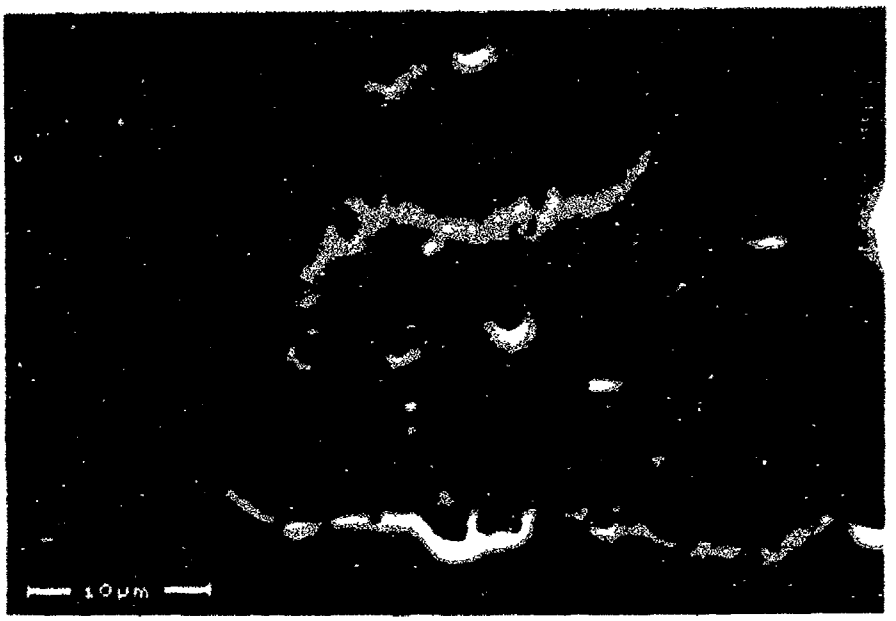

(A)

(B)

Figure 2. SEM micrographs revealing locations of coarse precipitates; (A) backscattered electron image of 8090 with Al-Li precipitates at boundaries, and (B) secondary electron image of Weldalite with Al-Cu-Fe precipitates at boundaries.

fracture toughness over 2519 Al, while providing an 8% reduction in density. The 8090 specimens did exhibit a significant reduction in ductility as well as a slight reduction in yield strength. The maximum compressive and tensile strengths of the 8090 alloy are very similar, with the exception of the short transverse orientations.

Weldalite plates demonstrated improvements of over 25% in yield strength, ultimate tensile strength and fracture toughness compared with 2519 Al, while providing a 3% reduction in density. The Weldalite displayed the highest shear strengths of the three Al-Li alloys and exhibited maximum compressive strengths well in excess of the tensile strengths for the respective specimen orientations.

Similar properties were observed for 2090-T8 plates where improvements of over 25% in yield strength and ultimate tensile strength, and also 10% in fracture toughness were obtained over 2519-T8 Al while providing a 7% reduction in density.[9,12,13] The only significant drawbacks of the 2090 alloy are the reduction in ductility and short transverse fracture toughness compared to 2519 Aluminum.

Table 2. MECHANICAL PROPERTIES

Alloy (Process)	Density ($lb/in.^3$)	Orient.	0.2% YS (ksi)	UTS (ksi)	Elong. (%)	K_{IC} ($ksi/\sqrt{in.}$)	σ_{comp} (ksi)	τ_{max} (ksi)
8090-T8771 (Extrusion)	0.093	L; L-T	60.0	70.7	3.9	31.0 *	71.5	40.6
		T; T-L	53.3	68.2	5.7	30.1 *	72.4	37.5
		S; S-L	48.7	63.9	7.3	22.4	81.2	
Weldalite-T8 (Plate)	0.099	L; L-T	81.2	88.2	12.5	33.5	109.7	49.3
		T; T-L	76.0	85.1	14.2	36.5 *	116.4	48.4
2090-T8E48 [13] (Plate)	0.094	L; L-T	81.0	84.9	8.5	30.5	71 †	46 †
		T; T-L	79.4	84.3	7.0	22.0	82 †	44 †
		S; S-L	63.8	71.2		16.9		
2519 -T87 [23] (Plate)	0.102	L; L-T	61.4	67.4	12.4	27.2		
		T; T-L	58.9	68.0	12.0	24.1		
		S; S-L				21.2		
5083 -H131 [23] (Plate)	0.096	L; L-T	46.2	54.7	9.3	30.3		
		T; T-L	41.7	56.8	12.7	27.6		

*: K_Q †: 2090-T81; Bucci et al. [9]

Axial fatigue properties of the Al-Li alloys are presented as S-N curves in Figure 3 in accordance with ASTM E 468-82, and are compared to 2090-T81 [9] and 2519-T87.[23] The curves are plotted to indicate the 50% survivability of the material The fatigue limit, S_f, is defined as the limit these curves attain as the specimens begin to runout. All three Al-Li alloys demonstrate significantly improved fatigue life over the 2519 aluminum alloys. The Weldalite, 2090 and 8090 alloys exhibit improvements in the fatigue limit of 150%, 100% and 50%, respectively over 2519. The relative

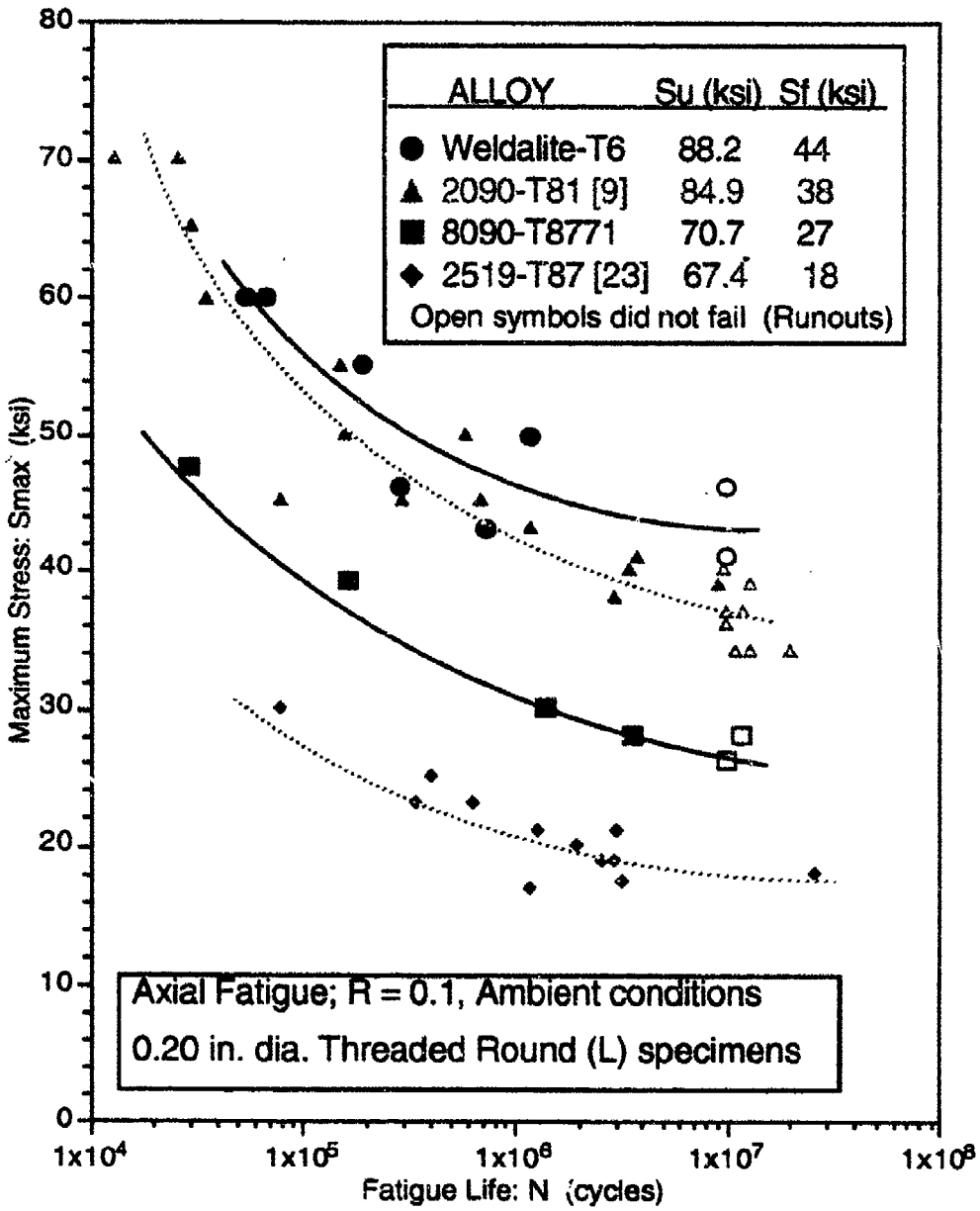

Figure 3. Smooth axial-stress fatigue (S-N) data for 8090-T8771, Weldalite-T6 and 2090-T81[9] aluminum-lithium alloys with respect to 2519-T87 aluminum.[23]

fatigue resistance of these alloys correlates very well with the ranking of the respective ultimate tensile strengths.

The 8090 L-T and T-L fracture toughness specimens failed to satisfy the sharp-crack tip condition established by ASTM E 399 for the size specimens utilized, specifying that:

$$a \text{ and } B < 2.5(K_Q/\sigma_{YS})^2$$

where a is the initial crack length, B is the specimen thickness and σ_{YS} is the 0.2% offset yield strength in the direction of the tensile axis. The conditional fracture toughness result (K_Q) is calculated from E 399-A4.5 for compact tension specimens. Although the specimens failed the criteria for a valid K_{IC} test, the fraction of oblique shear at the edges of the L-T and T-L specimens is minimal, such that the K_Q values presented should closely approximate the plane-strain condition. These criteria are satisfied for the larger S-L specimens, thus validating the K_{IC} values. For the Weldalite alloy, the plane-strain criteria are satisfied only for the L-T specimens.

2. Failure Mechanisms

The 8090 tensile specimens fractured under mixed modes of transgranular shear and intergranular failure, as depicted by the micrograph in Figure 4-A. Elongated primary grains failed by transgranular shear while recrystallized regions failed predominantly by an intergranular mechanism. Such mixed modes of failure are common in Al-Li alloys.[2,4,10,13,14] The mixed modes of failure are particularly prevalent in extruded Al-Li alloys, where the fracture mode progresses from intergranular to transgranular as the processing temperature compensated strain rate is decreased.[24] For underaged conditions, failure has been shown to occur primarily by transgranular shear as the S' and T_1 fractions are too low to prevent strain localization.[6,7,25] The coarsening of equilibrium precipitates at grain boundaries and the widening of PFZ's during over aging lead to extensive intergranular failure and a reduction in ductility.[2,7,25]

The presence of micro dimpling in the regions of transgranular shear can be observed in Figure 4-B. Transgranular shear with micro dimpling has been previously identified for peak and slightly overaged conditions in Al-Li alloys of compositions similar to 8090.[6] Some recrystallized grains were identified as failing in a brittle mode, initiating at Al-Li inclusions, as depicted in Figure 4-B. Secondary cracking was also noted in the recrystallized regions to follow paths rich in Al-Li precipitates. For other Al-Li alloys, secondary cracking has been attributed to the presence of coarse precipitates and the resulting PFZ's at subgrain boundaries.[25] Low ductility and fracture toughness in the short transverse direction are also attributed to weak boundaries in the rolling or extrusion plane.[26]

Weldalite tensile specimens also demonstrated mixed modes of failure as presented in Figure 5-A. Transgranular shear of primary grains and extensive microvoid coalescence initiating at clusters of Al-Cu-Fe precipitates were identified. Similar results have been observed in 2090 with microvoid coalescence around Cu_2FeAl_7 particles.[13] A closer examination indicates that the transgranular shear occurs along subgrains parallel to the rolling direction, and steps to adjacent subgrains. The BEI micrograph in Figure 5-B reveals that these steps are initiated by

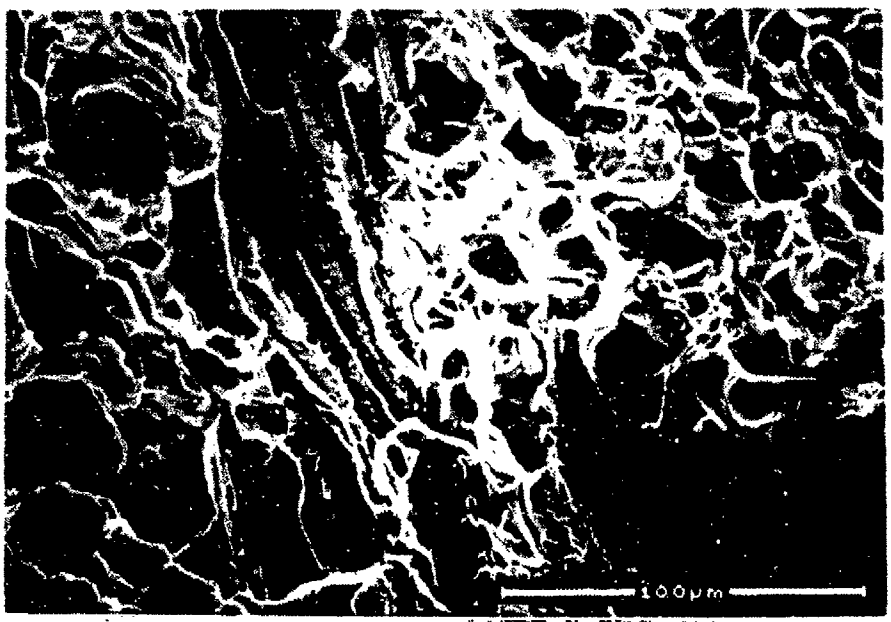

(A)

(B)

Figure 4. SEM micrographs depicting failure modes of 8090 tensile (L) specimens; (A) mixed modes of transgranular shear and intergranular failure, and (B) brittle fracture of recrystallized grain initiating at Al-Li precipitates.

(A)

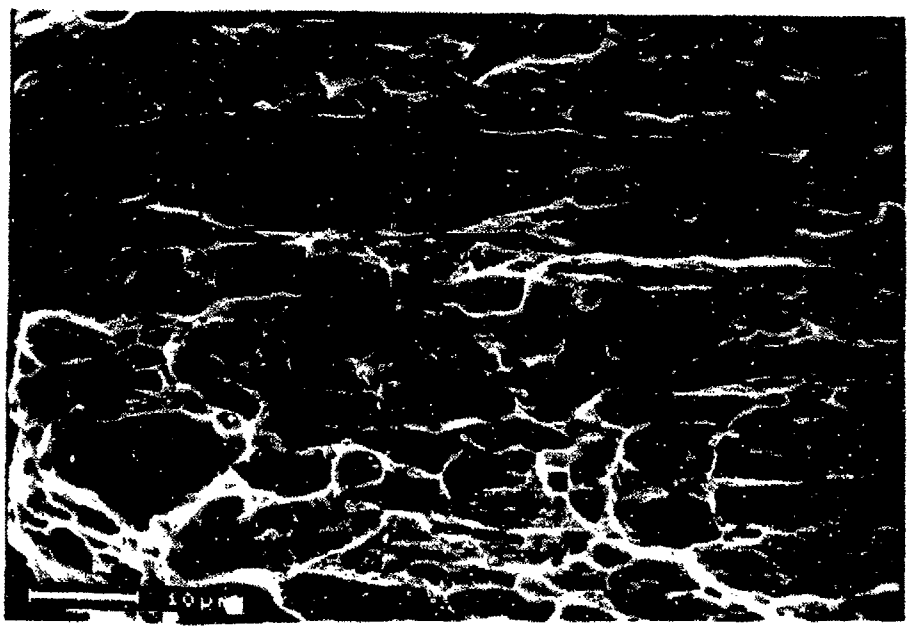

(B)

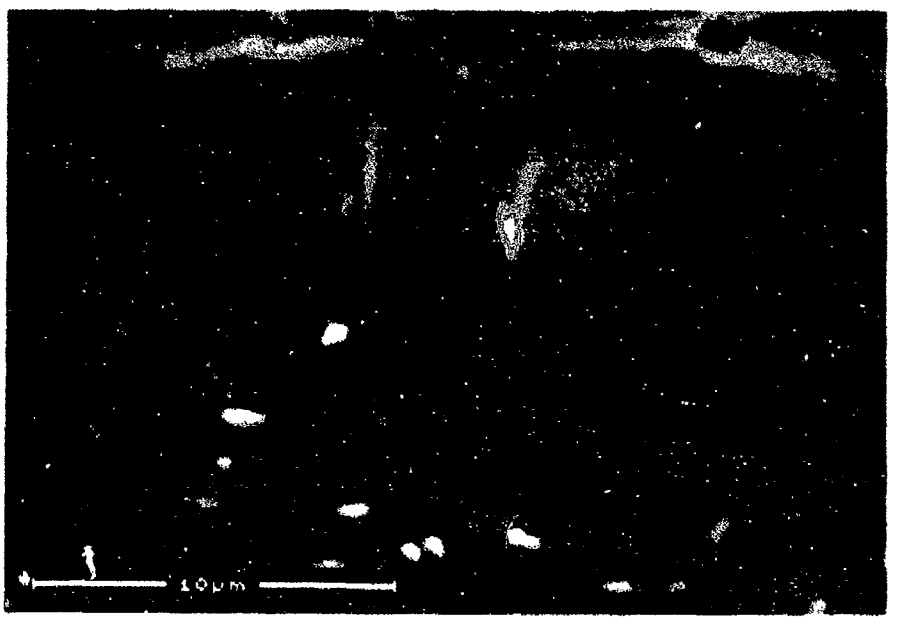

Figure 5. SEM micrographs depicting failure modes in Weldalite tensile (L) specimens; (A) mixed transgranular shear and ductile shear lips, and (B) microvoid coalescense at subgrain boundaries leading to steps.

multiple Al-Cu-Fe precipitates. Failure in Al-Li alloys has been shown to occur predominantly along grain boundaries parallel to the rolling direction with steps to adjacent planes. These steps initiate at intersecting grain boundaries and shear bands by a ductile failure mechanism.[26] Many of the recrystallized grains in Weldalite failed in a brittle manner, also initiating at multiple Al-Cu-Fe precipitates.

Dynamic Behavior

1. Ballistic Properties

Both 8090 extrusions and Weldalite plates provided enhanced ballistic performance over 2519 and 5083 Al alloys. The V_{50} ballistic limits against AP and FSP projectiles at 0° obliquity are plotted versus armor demand in Figures 6 and 7, respectively. The armor demand is emperically derived as the areal density, ρ_A (lb/ft^2), divided by the projectile diameter, d (in.):

$$\text{armor demand} = \frac{\rho_A / d \quad (lb/ft^2)}{in.}$$

The areal density is defined as is the target thickness, t (ft), multiplied by the density of the alloy, ρ (lb/ft^3):

$$\rho_A = t \cdot \rho \quad (lb/ft^2)$$

For a given material, the ballistic data for different caliber projectiles superimpose on single curves for either AP or FSP projectiles when plotted against armor demand. This technique allows designers to evaluate ballistic performance as a function of projectile type rather than for individual caliber munitions. The AP and FSP projectile diameters are included as inserts in the plots. Ballistic data for 2519 and 5083 are included as the high and low ends of aluminum alloys currently being considered for structural armor applications.[27]

Against AP projectiles (Figure 6), the Weldalite plates consistently demonstrated ballistic limits (V_{50}) about 10% in excess of the mean values for the 2519 aluminum alloy. Data for Weldalite plates supplied by the manufacturer also agrees with this trend.[28] The 8090 extrusions demonstrated V_{50} data slightly lower than the mean values for 2519, while 8090 plates[29] yielded ballistic limits just above the 2519. The dynamic performance of these alloys under ballistic testing correlates with the ranking of yield strengths obtained under static loading rates in Table 2. Against the FSP projectiles (Figure 7), there appeared to be little difference between the Al-Li and aluminum alloys. The 2090-T8E48 Al-Li alloy also demonstrates similar ballistic limits against the FSP projectiles.[13]

2. Failure Mechanisms

Figures 8-A and B indicate that penetration of 12.7 mm FSP projectiles resulted in mixed modes of dynamic failure by plugging and delamination mechanisms. These optical micrographs display penetration cross-sections still containing the plugs. Upon impact by a blunt projectile (FSP), strong compressive waves propagate through the target and reflect as tensile waves.[30] Failure generally occurs as the intensity of the tensile wave exceeds the dynamic ultimate tensile strength of the

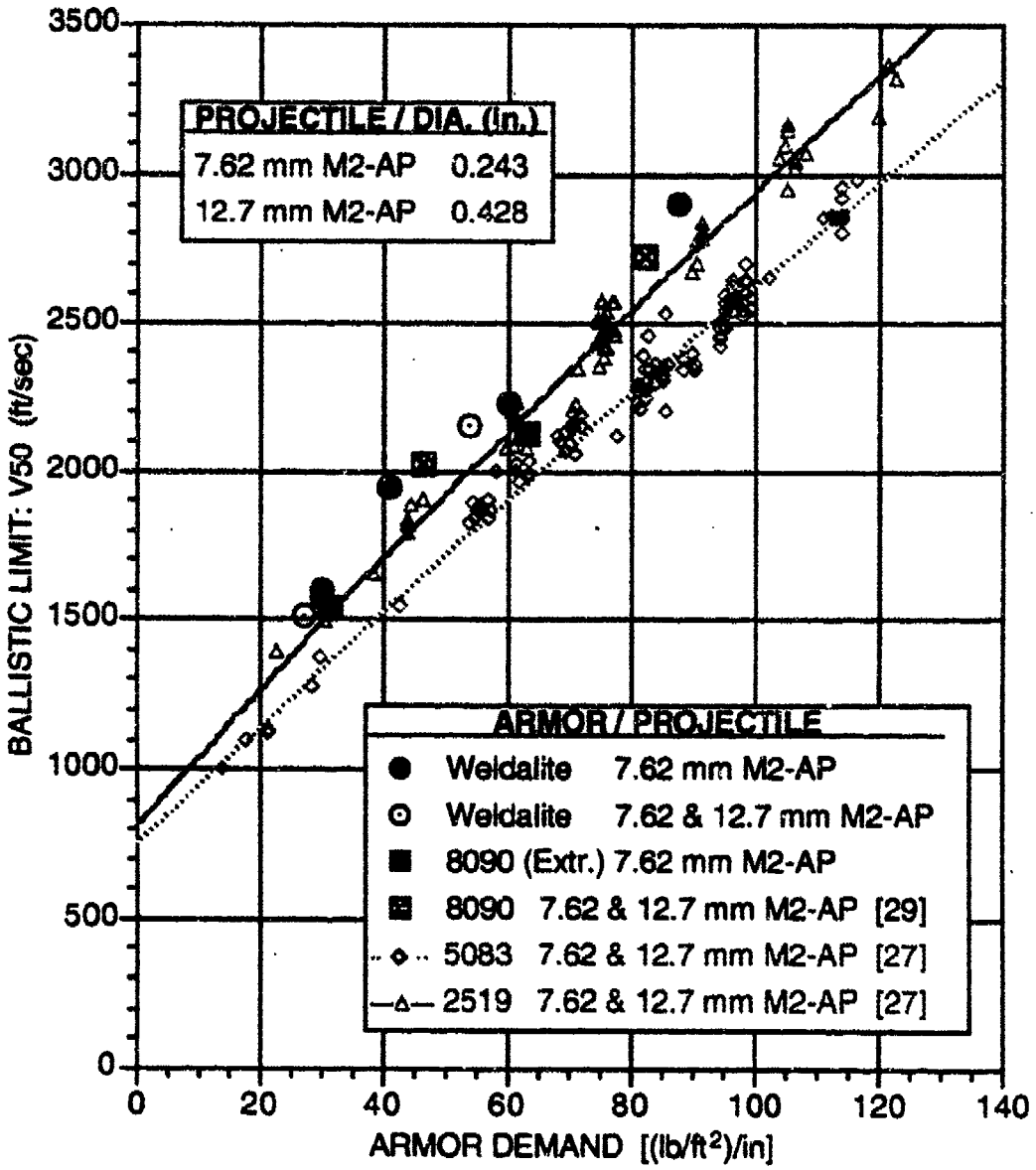

Figure 6. Ballistic limit (V_{50}) versus armored demand at 0° obliquity against armor piercing projectiles.

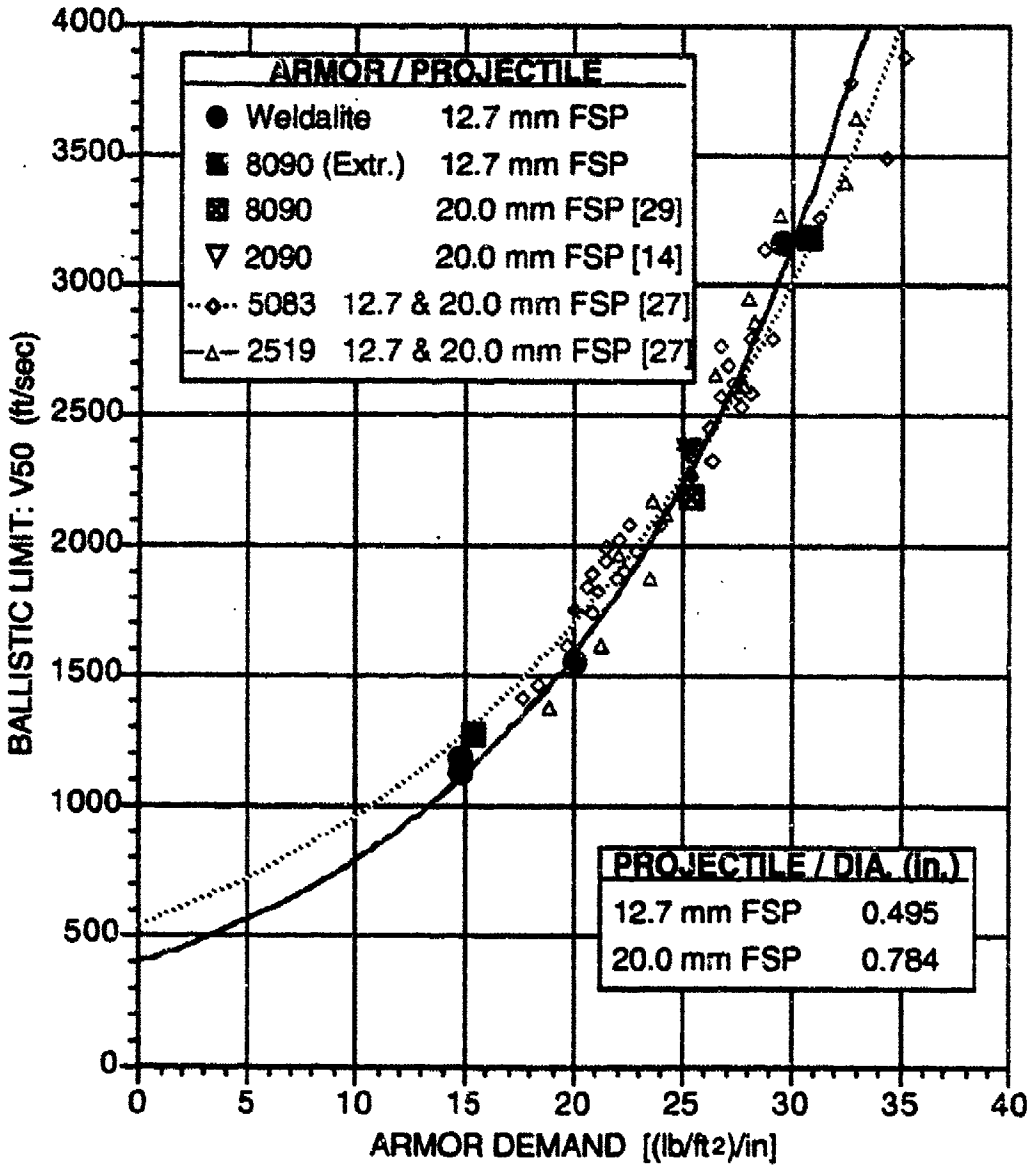

Figure 7. Ballistic limit (V_{50}) versus armor demand at 0° obliquity against fragment simulating projectiles (FSP).

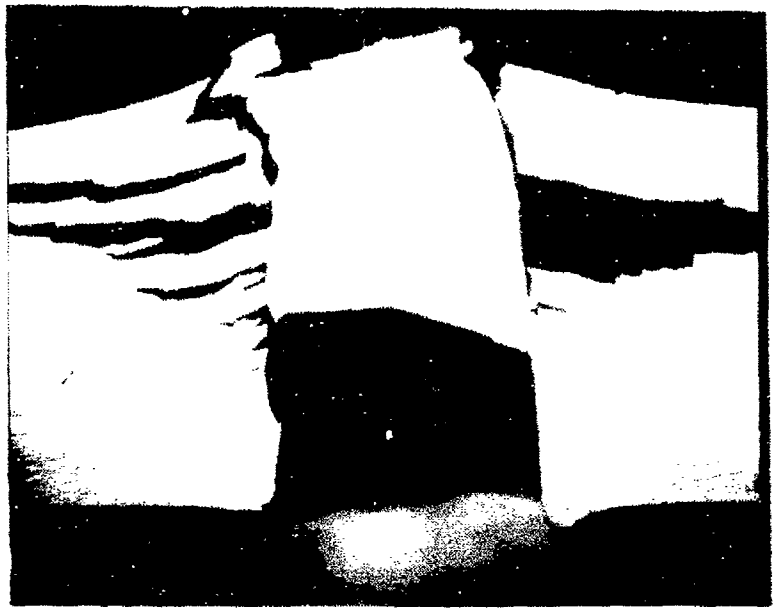

(A)

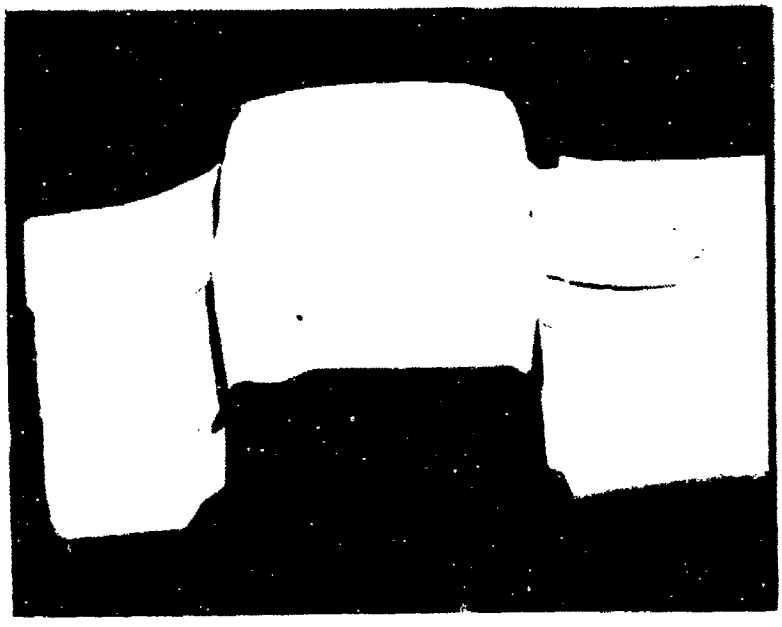

(B)

Figure 8. Optical micrographs of 12.7-mm FSP penetration cross sections at lower projectile velocities; (A) plugging and delamination of 8090 extrusion, and (B) plugging and stepped cracking of Weldalite plate.

material. In aluminum alloys, plugging is attributed to narrow bands of intense plastic strain along planes of maximum shear stress or minimum strength.

The cross-section of the 8090 specimen in Figure 8-A displays significant delamination initiating at the plug interface and extending in the longitudinal and transverse directions. Higher projectile velocities and thicker 8090 targets, lead to increased delamination as the projectile exited the material. Extensive delamination was also obtained in ballistic testing of 2090-T8E48 plates.[13] In overaged conditions, delamination of 8090 flat tensile specimens with polished surfaces were identified as initiating at grain boundary precipitates.[30]

The cross-section of the Weldalite specimen in Figure 8-B reveals substantially less delamination although the presence of stepped cracks at a 45° angle from the projectile axis can be observed. This is similar to the failure mechanism identified under static testing where fracture occurred along boundaries parallel to the rolling plane and stepped to boundaries on adjacent planes. For thicker Weldalite targets, stepped cracks propagated to the surface, resulting in spalling. Spalling is known to occur primarily in materials that demonstrate compressive strengths well in excess of the ultimate tensile strengths.[31] Such a difference was obtained for Weldalite under static loading conditions as observed in Table 2.

Examination of the spalled and delaminated fracture surfaces by SEM reveals some differences in failure mechanisms between dynamic and static testing conditions. Both Al-Li alloys still exhibit extensive areas of flat transgranular shear but Figures 9-A and B also reveal an intersubgranular failure mode along low angle boundaries. In addition, the Weldalite spalled surface demonstrates a stepping of the transgranular shear between adjacent grains parallel to the rolling plane.

CONCLUSIONS

1. Both 8090-T8771 and Weldalite-T8 Al-Li alloys demonstrate superior strength to weight ratios compared to the 2519-T87 and 5083-H131 aluminum alloys. The 8090 possesses comparable mechanical properties while providing an 8% reduction in density over 2519. The Weldalite has a comparable density as 2519 but demonstrates improvements of over 25% in yield strength, ultimate tensile strength and fracture toughness.

2. The two Al-Li alloys display significantly improved axial fatigue properties over 2519-T87 and 5083-H131 aluminum plates. The Weldalite plates and 8090 extrusions demonstrated an increase in excess of 150% and 50%, respectively, in the fatigue limit compared to 2519.

3. Both 8090 and Weldalite provide ballistic properties comparable to the 2519 and 5083 aluminum alloys against both AP and FSP projectiles. Both Al-Li alloys fall within the range of scatter for the 2519 alloy, yet above the range of the 5083 data.

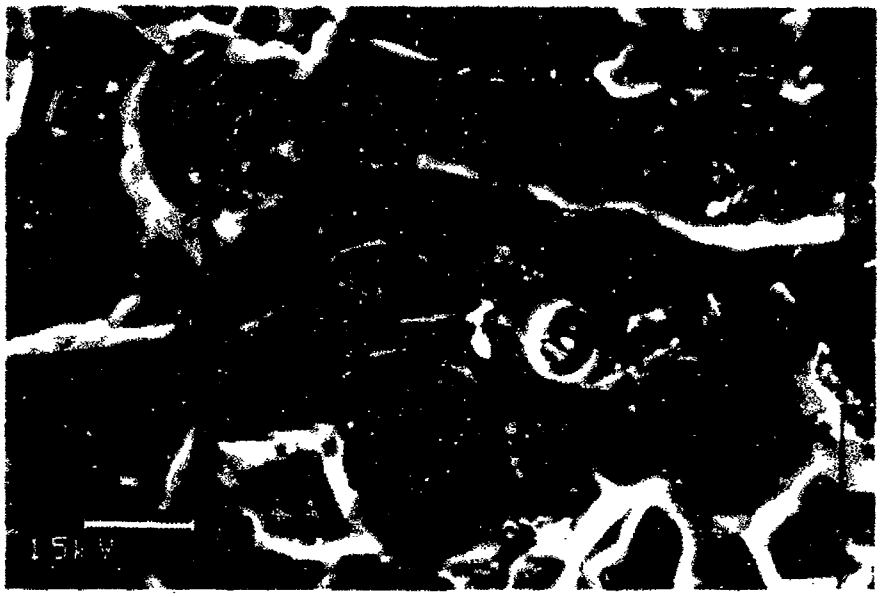

(A)

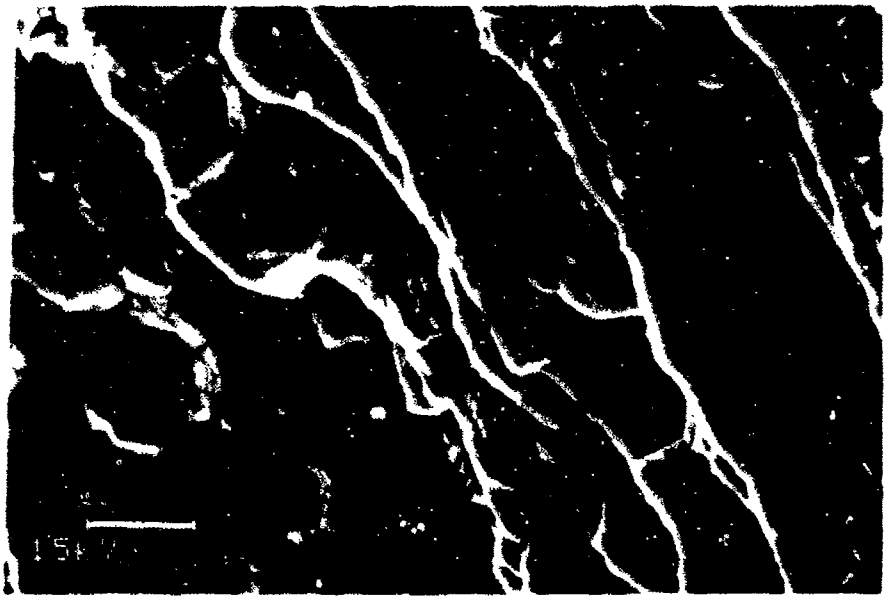

(B)

Figure 9. SEM micrographs of fracture surfaces of ballistic targets revealing transgranular shear with intersubgranular failure along low angle boundaries; (A) 8090 delamination fracture surface, and (B) Weldalite spall fracture surface.

RECOMMENDATIONS

Whether the goal is to reduce weight or to improve strength, Al-Li alloys offer significant potential for replacing alloys such as 2519 and 5083 as light-weight, high-strength structural armor materials. The limited ballistic data of this study indicates that these Al-Li alloys possess ballistic limits equal to or greater than what is currently being considered for aluminum armor materials. Establishment of a more extensive data base on the ballistic performance as well as optimization of factors that minimize plugging, delamination or spalling is strongly recommended.

APPENDIX A. 8090 TESTING DATA

Appendix A.1 8090 Tensile Testing

8090 Extrusion T-8771

Tensile Testing
ASTM B 557: Tension Testing Wrought and Cast Aluminum- and Magnesium-Alloy Products.
Equipment: 20 KIP Electromechanical Tension/Compression Machine
Load Cell: 5,000 lb (1,000 lb for [S] specimens)
Cross-Head: 0.02 in/min
Strain Gages: 1" 10% for [L] and [T] specimens, 0.5" 10% for [S] specimens

Specimen	Diameter (in.)	0.2% YS (ksi)	UTS (ksi)	Elongation (%)	Modulus (Msi)	Remarks
L-1	0.250	69.6	76.0	2.8	10.9	(a)
L-2	0.250	57.5	68.8	3.2	11.0	(a)
L-3	0.250	58.0	70.8	4.7	11.3	(a)
L-4	0.250	58.0	69.8	5.2	11.1	
L-5	0.250	59.0	69.4	3.4	10.8	(a)
L-6	0.250	58.0	69.4	4.1	11.3	
T-1	0.250	52.8	68.2	6.3	11.0	(a)
T-2	0.250	53.8	68.4	5.0	10.8	(a)
T-3	0.250	53.0	68.6	6.5	10.6	
T-4	0.250	52.5	68.0	6.5	10.3	
T-5	0.250	54.0	67.5	4.1	11.0	(a)
T-6	0.250	53.5	68.5	5.9	10.8	(a)
S-1	0.100	51.0	66.5	6.0	9.9	
S-2	0.100	43.0	58.3	8.0	9.6	
S-3	0.100	52.0	67.0	8.0	9.8	(b)
Summary:						
L	0.250	60.0	70.7	3.9	11.1	
T	0.250	53.3	68.2	5.7	10.8	
S	0.100	48.7	63.9	7.3	9.8	

Remarks:
(a): Specimen failure initiated at gage mark indentation.
(b): Specimen failed outside gage mark.

Appendix A.2 8090 Compression Testing

8090 T-8771 Extrusion

Compression Testing
ASTM E 9: Compression Testing of Metallic Materials at Room Temperature.

Equipment: 20 KIP Electromechanical Tension/Compression Machine
Load Cell: 20,000 lb
Cross-Head: 0.1 in/min

Specimen	Diameter (in.)	Length (in.)	0.2% YS (ksi)	Compressive (ksi)	Modulus (Msi)	Remarks
L-1	0.50	1.499	65.3	73.5	10.6	
L-2	0.50	1.500	54.6	75.5	10.4	
L-3	0.50	1.499	53.8	72.7	11.1	
L-4	0.50	1.500	61.7	69.9	9.9	
L-5	0.50	1.500	52.8	67.9	11.9	
L-6	0.51	1.497	53.9	69.6	10.8	
T-1	0.50	1.500	58.2	73.0	9.5	
T-2	0.50	1.495	59.9	73.7	11.9	
T-3	0.51	1.500	58.8	66.7	13.4	
T-4	0.51	1.499	55.7	67.6	11.8	
T-5	0.51	1.499	58.1	79.4	11.3	
T-6	0.51	1.501	64.7	73.8	8.9	
S-1	0.51	1.497	51.5	75.7	10.1	
S-2	0.50	1.495	52.0	79.1	11.2	
S-3	0.50	1.503	52.0	88.8	11.5	(a)
SUMMARY:						
L	0.50	1.499	57.0	71.5	10.8	
T	0.51	1.499	59.2	72.4	11.1	
S	0.50	1.498	51.8	81.2	10.9	

Remarks:

(a): Specimen failed by shear. All other specimens buckled, and tests were terminated after a 5% drop in load was observed. Compressive strengths then determined from maximum load.

Appendix A.3 8090 Shear Testing

8090 T-8771 Extrusion

Shear Testing
ASTM B 565: Shear Testing of Aluminum and Aluminum-Alloy Rivets and Cold-Heating Wire and Rods.

Equipment: 50 KIP Electromechanical Tension/Compression Machine
Load Cell: 20,000 lb
Cross-Head: 0.1 in./min

Specimen	Diameter (in.)	Max Load (lbf)	Max Shear (ksi)	Remarks
L-1	0.499	15,900	40.7	
L-2	0.499	16,200	41.4	
L-3	0.499	17,590	45.0	(a)
L-4	0.499	15,500	39.6	
L-5	0.499	16,200	41.4	
L-6	0.499	15,590	39.9	
T-1	0.500	15,050	38.3	
T-2	0.499	14,650	37.5	
T-3	0.499	13,890	35.5	
T-4	0.500	15,200	38.7	
T-5	0.500	14,900	38.0	
T-6	0.499	14,400	36.8	
SUMMARY:				
L	0.499	16,163	40.6	
T	0.500	14,682	37.5	

Remarks:

Max Shear = $P_{max}/2A$

All specimens sheared on two planes along the compressive axis.

(a): possible bushing interference.

Appendix A.4 8090 Fracture Toughness Testing

8090 T-8771 Extrusion

Fracture Toughness
ASTM E 399 Plane-Strain Fracture Toughness of Metallic Materials.

Compact Tension Specimens
Size: L-T & T-L specimens: W= 1.00 in., B= 0.50 in.
S-L specimens: W= 1.50 in., B= 0.75 in.
Equipment: 10 KIP Servo-hydraulic testing machine
Cross-Head: 0.1 in./min
Precracked: According to ASTM E 399 Annex 4
Plane-Strain Criteria:

(a) $0.45 < (a/W) < 0.55$

(b) a & B $> 2.5(K_Q/\sigma_{YS})^2$, where σ_{YS} from 8090 Tensile test (Appendix A.1) :
L: 60.0 ksi; T: 53.3; S: 48,7

(c) $P_{max}/P_Q < 1.10$

Specimen	a (in.)	a/W	Pmax/Pq	K_Q (lb/$\sqrt{in.}$)	$2.5(K_Q/\sigma_{YS})^2$	Remarks
LT-2	0.521	0.521	1.00	31.85	0.704	(b)
LT-3	0.529	0.529	1.07	32.92	0.753	(b)
LT-5	0.527	0.527	1.01	30.15	0.631	(b)
LT-6	0.532	0.532	1.02	28.98	0.583	(b)
TL-1	0.523	0.523	1.17	29.84	0.784	(b), (c)
TL-3	0.533	0.533	1.19	28.86	0.733	(b), (c)
TL-4	0.514	0.514	1.14	30.75	0.832	(b), (c)
TL-5	0.541	0.541	1.18	30.19	0.802	(b), (c)
TL-6	0.522	0.522	1.16	30.85	0.838	(b), (c)
SL-1	0.741	0.494	1.00	22.60	0.538	K_{IC}
SL-2	0.715	0.477	1.01	22.60	0.538	K_{IC}
SL-3	0.737	0.491	1.02	22.70	0.543	K_{IC}
SL-4	0.738	0.492	1.02	22.40	0.529	K_{IC}
SL-5	0.754	0.503	1.01	22.30	0.524	K_{IC}
SL-6	0.713	0.475	1.04	21.50	0.487	K_{IC}
SUMMARY:						
LT	0.527	0.527	1.03	30.98	0.668	K_Q
TL	0.527	0.527	1.17	30.10	0.798	K_Q
SL	0.733	0.489	1.02	22.35	0.527	K_{IC}

Remarks:

Letters refer to plane-strain criterion that are invalid.
TL-2 did not align with fixture, LT-1 and LT-4 specimens failed during loading.

8090 T-8771 Extrusion

Axial Fatigue
ASTM E 466 Conducting Constant Amplitude Axial Fatigue Tests of Metallic Materials.

Equipment: Rotating Mass testing machine
Stress Ratio: R = 0.1
Frequency: 30 Hz
Conditions: Ambient temperature and humidity

Specimen	Diameter (in.)	Max Stress (ksi)	Cycles	Remarks
L-1	0.199	26.2	10,382,000	(a)
L-2	0.199	28.0	3,639,000	
L-3	0.200	27.8	171,000	
L-4	0.199	30.1	1,411,000	
L-5	0.201	39.3	164,000	
L-6	0.200	47.5	30,000	
L-7	0.199	27.5	11,787,000	(a)
L-8	0.199	37.5	-	(b)

Remarks:
(a) Specimen Run out in excess of 10,000,000 cycles.
(b) Specimen failed from a galled thread while being installed in the test machine.

APPENDIX B. WELDALITE TESTING DATA

Appendix B.1 Weldalite Tensile Testing

Weldalite T-8 Plates

Tensile Testing
ASTM B 557: Tension Testing Wrought and Cast Aluminum- and Magnesium-Alloy Products.
Equipment: 20 KIP Electromechanical Tension/Compression Machine
Load Cell: 5,000 lb.
Cross-Head: 0.02 in./min
Strain Gages: 1" 10% for [L] and [T] specimens.

Specimen	Diameter (in.)	0.2% YS (ksi)	UTS (ksi)	Elongation (%)	Modulus (Msi)	Remarks
L-1	0.249	81.9	88.6	12.9	10.8	(a)
L-2	0.251	81.3	88.2	11.7	10.9	(a)
L-3	0.252	80.4	87.7	12.9	10.4	(a)
T-1	0.249	75.4	84.7	14.1	10.8	(b)
T-2	0.250	76.8	85.6	13.6	10.2	(b)
T-3	0.249	75.7	84.9	15.0	10.7	(a)
SUMMARY:						
L	0.250	81.2	88.2	12.5	10.7	
T	0.250	76.0	85.1	14.2	10.6	

Remarks:

ASTM B 557 recommends not to compare values of % Elongation for subsized specimens.

(a) Specimens sheared at a 45° angle to the tensile axis.

(b) Specimens sheared along two planes intersecting to form a "V" surface.

Appendix B.2 Weldalite Compression Testing

Weldalite T-8 Plates

Compression Testing
ASTM E 9: Compression Testing of Metallic Materials at Room Temperature.

Equipment: 50 KIP Electromechanical Tension/Compression Machine
Load Cell: 50,000 lb
Cross-Head: 0.1 in./min

Specimen	Diameter (in.)	Length (in.)	Compressive (ksi)	Remarks
L-1	0.499	1.500	111.2	
L-2	0.496	1.500	107.2	
L-3	0.494	1.500	110.7	
T-1	0.495	1.500	115.4	
T-2	0.496	1.500	119.0	
T-3	0.497	1.500	114.7	(a)
SUMMARY:				
L	0.496	1.500	109.7	
T	0.496	1.500	116.4	

Remarks:

(a): Specimen failed by shear. All other specimens buckled, and tests were terminated after a 5% drop in load was observed. Compressive strengths then determined from maximum load.

Appendix B.3 Weldalite Shear Testing

Weldalite T-8 Plate

Shear Testing
ASTM B 565: Shear Testing of Aluminum and Aluminum-Alloy Rivets and Cold-Heating Wire and Rods.

Equipment: 50 KIP Electromechanical Tension/Compression Machine
Load Cell: 50,000 lb
Cross-Head: 0.1 in./min

Specimen	Diameter (in.)	Max Load (lbf)	Max Shear (ksi)	Remarks
L-1	0.498	19,300	49.5	(a)
L-2	0.498	19,050	48.8	(a)
L-3	0.498	19,375	49.7	(a)
T-1	0.498	19,100	49.0	
T-2	0.497	18,800	48.5	
T-3	0.498	18,600	47.7	
SUMMARY:				
L	0.498	19,242	49.3	
T	0.498	18,833	48.4	

Remarks:

Max Shear = $P_{max}/2A$

(a) Specimens sheared on two planes along the compressive axis.

Appendix B.4 Weldalite Fracture Toughness Testing

Weldalite T-8 Plate

Fracture Toughness
ASTM E 399 Plane-Strain Fracture Toughness of Metallic Materials.

Compact Tension Specimens
Size: L-T & T-L specimens: W= 1.00 in., B= 0.50 in.
Equipment: 10 KIP Servo-hydraulic testing machine
Cross-Head: 0.1 in./min
Precracked: According to ASTM E 399 Annex 4
Plane-Strain Criteria:

(a) $0.45 < (a/W) < 0.55$

(b) $a \& B > 2.5(K_Q/\sigma_{YS})^2$, where σ_{YS} from Weldalite Tensile test (Appendix B.1) : L: 81.2 ksi; T: 76.0

(c) $P_{max}/P_Q < 1.10$

Specimen	a (in.)	a/W	P_{max}/P_Q	K_Q (lbs./$\sqrt{in.}$)	$2.5(K_Q/\sigma_{YS})^2$	Remarks
LT-1	0.481	0.481	1.05	26.83	0.273	K_{IC}
LT-2	0.503	0.503	1.18	37.28	0.527	(b), (c)
LT-3	0.526	0.526	1.15	33.34	0.421	(c)
LT-4	0.430	0.430	1.27	36.39	0.502	(b), (c)
LT-5	0.480	0.480	-	-	-	
LT-6	0.487	0.487	1.14	33.70	0.431	(c)
TL-1	0.477	0.477	1.38	40.15	0.698	(b), (c)
TL-2	0.457	0.457	1.09	35.63	0.549	(b)
TL-3	0.502	0.502	1.15	34.96	0.529	(b), (c)
TL-4	0.461	0.461	1.13	35.86	0.557	(b), (c)
TL-5	0.458	0.458	1.12	36.91	0.590	(b), (c)
TL-6	0.456	0.456	1.09	35.51	0.546	(b)
SUMMARY:						
LT	0.484	0.484	1.16	33.51	0.431	
TL	0.469	0.469	1.16	36.50	0.578	

Remarks:
Letters refer to plane-strain criteria that are invalid
Specimen LT-5 failed prior to loading.

Appendix B.5 Weldalite Fatigue Testing

Weldalite T-8 Plate

Axial Fatigue
ASTM E 466 Conducting Constant Amplitude Axial Fatigue Tests of Metallic Materials.

Equipment: 10 KIP Servo-hydraulic testing machine
Stress Ratio: R = 0.1
Frequency: 10 Hz
Conditions: Ambient temperature and humidity

Specimen	Diameter (in.)	Max Stress (ksi)	Cycles	Remarks
L-1	0.199	60	67,580	
L-2	0.199	50	1,205,760	
L-3	0.199	46	290,042	
L-4	0.202	40	10,010,000	(a)
L-5	0.202	43	754,000	
L-6	0.199	46	10,026,880	(a)
L-7	0.199	55	191,520	
L-8	0.199	60	54,220	

Remarks:
(a) Specimen Run out in excess of 10,000,000 cycles.

REFERENCES

1. SANDERS, T. H., Jr. and STARKE, E. A., Jr., *Acta Met.*, Vol. 30, 1982, p. 927.

2. DOORBAR, P.J. , BORRADAILE, J.B., and DRIVER, D., *Evaluation of Aluminium-Lithium-Copper-Magnesium-Zirconium Alloy as a Forging Material*, Aluminium-Lithium Alloys III, Ed. by C. Baker, The Institute of Metals, 1986, p. 496.

3. TOSTEN, M. A., VASUDEVAN, A. K., and HOWELL, P. R., *Grain Boundary Precipitation in Al-Li-Cu Alloys*, Aluminium-Lithium Alloys III, Ed. by C. Baker, The Institute of Metals, 1986, p. 490.

4. ASHTON, R. F., THOMPSON, D. S., STARKE, E. A.,Jr., and LIN, F. S., *Processing Al-Li-Cu-(Mg) Alloys*, Aluminium-Lithium Alloys III, Ed. by C. Baker, The Institute of Metals, 1986, p. 66.

5. TOSTEN, M. H., VASUDEVAN, A. K. and HOWELL, P. R., *Microstructural Development in Al-2%Li-3%Cu Alloy*, Aluminium-Lithium Alloys III, Ed. by C. Baker, The Institute of Metals, 1986, p. 483.

6. AHMAD, M. and ERICSSON, T., *Coarsening of δ', T1, S' Phases and Mechanical Properties of Two Al-Li-Cu-Mg Alloys*, Aluminium-Lithium Alloys III, Ed. by C. Baker, The Institute of Metals, 1986, p. 509.

7. MEYER, P. and DUBOST, B., *Production of Aluminium-Lithium Alloy with High Specific Properties*, Aluminium-Lithium Alloys III, Ed. by C. Baker, The Institute of Metals, 1986, p. 37.

8. "Metals- Mechanical Testing; Elevated and Low-Temperature Tests; Metallography", Metals Test Methods and Analytical Procedures, Annual Book of ASTM Standards, Vol. 03.01, ASTM, Philadelphia, PA, 1992.

9. BUCCI, R. J., MALCOLM, R. C., COLVIN, E. L., MURTHA, S. J., and JAMES, R. S., *Cooperative Test Program for the Evaluation of Engineering Properties of Al-Li Alloy 2090-T8X Sheet, Plate, and Extrusion Products*, Naval Surface Warfare Center, NSWC TR 89-106, September 1989.

10. LAVERNIA, E. J., SRIVATSAN, T. S., and MOHAMED, F. A., *Strength, Deformation, Fracture Behavior and Ductility of Aluminium-Lithium Alloys*, *J. Mater. Sci.*, **25**, 1990, p. 1137.

11. PICKENS, J. R., HEUBAUM, F. H., LANGAN, T. J., and KRAMER, L. S., *Al--4.5-6.3 Cu--1.3 Li--0.4 Ag--0.4 Mg--0.14 Zr Alloy Weldalite™ 049*, Aluminum-Lithium Alloys- 5, Ed. by T. H. Sanders Jr. and E. A. Starke Jr., Materials and Component Engineering Publications Ldt., Birmingham, UK, 1989, p. 1397.

12. BRETZ, P. E. and SAWTELL, R. R., *'Alithite' Alloys: Progress, Products and Properties*, Aluminium-Lithium Alloys III, Ed. by C. Baker, The Institute of Metals, 1986, p. 47.

13. CHIN, E. S. C., CAPPUCCI, M. R., HUIE, R. M., and PASTERNAK, R. E., *Evaluation of 2090-T8E48 Aluminum-Lithium Plates*, U.S. Army Materials Technology Laboratory, MTL TR 89-97, November 1989.

14. BUSCEMI, C. D. and CHIN, E. S. C., *Characterization of X2090 Al-Li Alloy*, U.S. Army Materials Technology Laboratory, MTL TR 88-26, September 1988.

15. REYNOLDS, M. A., GRAY, A., CREED, E., JORDAN, R. M., and TITCHENER, A. P., *Processing and Properties of Alcan Medium and High Strength Al-Li-Cu-Mg Alloys in Various Product Forms*, Aluminium-Lithium Alloys III, Ed. by C. Baker, The Institute of Metals, 1986, p. 57.

16. BULL, M. J. and LLOYD, D. J., *Textures Developed in Al-Li-Cu-Mg Alloy*, Aluminium-Lithium Alloys III, Ed. by C. Baker, The Institute of Metals, 1986, p. 402.

17. WERT, J. A., *Thermomechanical Processing of Heat-Treatable Aluminum Alloys for Grain Size Control*, Microstructural Control in Aluminum Alloys: Deformation, Recovery and Recrystallization, Ed. by E. H. Chia and H. J. McQueen, The Metallurgical Society, 1986, p. 67.

18. LLOYD, D.J., *The Influence of Particles and Deformation Structure on Recrystallization*, Microstructural Control in Aluminum Alloys: Deformation, Recovery and Recrystallization, Ed. by E. H. Chia and H. J. McQueen, The Metallurgical Society, 1986, p. 45.

19. WILLIAMS, J. C. and STARKE, E. A., Jr., *The Role of Thermomechanical Processing in Tailoring the Properties of Aluminum and Titanium Alloys*, Deformation Processing and Structure, Ed. by G. Krauss, Americal Society of Metals, 1982, p. 279.

20. BALL, M. D. and LAGACE, H., *Characterization of Coarse Precipitates in Overaged Al-Li-Cu-Mg Alloy*, Aluminium-Lithium Alloys III, Ed. by C. Baker, The Institute of Metals, 1986, p. 555.

21. MALIS, T., *Characterization of Lithium Distribution in Aluminum Alloys*, Aluminium-Lithium Alloys III, Ed. by C. Baker, The Institute of Metals, 1986, p. 347.

22. GU, B. P., MAHALINGHAM, K., LIEDL, G. L., and SANDERS, T. H.,Jr., *The δ' (Al3Li) Particle Size Distributions in a Variety of Al-Li Alloys*, Aluminium-Lithium Alloys III, Ed. by C. Baker, The Institute of Metals, 1986, p. 360.

23. DELUCA, E. and ANCTIL, A., *Laminate Armor for Light Combat Vehicles*, U.S. Army Materials Technology Laboratory, MTL TR 86-14, April 1986.

24. SHEPPARD, T., ZARDI, M. A., TUTCHER, M.G., and PATERSON, N.C., *On the Development of Structure During the Extrusion Process*, Microstructural Control in Aluminum Alloys: Deformation, Recovery and Recrystallization, Ed. by E. H. Chia and H. J. McQueen, The Metallurgical Society, 1986, p. 123.

25. JATA, K. V. and STARKE, E. A.,Jr., *Fatigue Crack Growth and Fracture Toughness Behavior of Al-Li-Cu Alloy*, Aluminium-Lithium Alloys III, Ed. by C. Baker, The Institute of Metals, 1986, p. 247.

26. MILLER, W. S., THOMAS, M. P., LLOYD, D. J., and CREBER, D., *Deformation and Fracture in Al-Li Base Alloys*, Aluminium-Lithium Alloys III, Ed. by C. Baker, The Institute of Metals, 1986, p. 584.

27. AMOS, C., Unpublished Research, U.S. Army Materials Technology Laboratory.

28. PICKENS, J. R., *Weldalite™ Alloys for Ground Vehicles*, Technical Data Package, Martin Marietta Laboratories, Baltimore, MD.

29. WANG, W. and BECK, J., Unpublished Research, U.S. Army Materials Technology Laboratory.

30. VERDU, C., GENTZBITTEL, J. M., and FOUGERES, R., *A Microstructural Study of Intergranular Fracture in a 8090 Al-Li Alloy*, Aluminum-Lithium Alloys-5, Ed. by T. H. Sanders Jr. and E. A. Starke Jr., Materials and Component Engineering Publications Ldt., Birmingham, UK, 1989, p. 899.

31. ZUKAS, J. A., *Penetration and Perforation of Solids*, Impact Dynamics, Ed. by J. A. Zukas, T. Nicholas, H. F. Swift, L. B. Grerszcuk, and D. R. Curran,John Wiley & Sons, Inc., New York, 1982, p. 155.

DISTRIBUTION LIST

No. of Copies	To
1	Office of the Under Secretary of Defense for Research and Engineering, The Pentagon, Washington, DC 20301
	Commander, U.S. Army Laboratory Command, 2800 Powder Mill Road, Adelphi, MD 20783-1145
1	ATTN: AMSLC-IM-TL
1	AMSLC-CT
	Commander, Defense Technical Information Center, Cameron Station, Building 5, 5010 Duke Street, Alexandria, VA 22304-6145
2	ATTN: DTIC-FDAC
1	MIA/CINDAS, Purdue University, 2595 Yeager Road, West Lafayette, IN 47905
	Commander, Army Research Office, P.O. Box 12211, Research Triangle Park, NC 27709-2211
1	ATTN: Information Processing Office
	Commander, U.S. Army Materiel Command, 5001 Eisenhower Avenue, Alexandria, VA 22333
1	ATTN: AMCSCI
	Commander, U.S. Army Materiel Systems Analysis Activity, Aberdeen Proving Ground, MD 21005
1	ATTN: AMXSY-MP, H. Cohen
	Commander, U.S. Army Missile Command, Redstone Scientific Information Center, Redstone Arsenal, AL 35898-5241
1	ATTN: AMSMI-RD-CS-R/Doc
1	AMSMI-RLM
	Commander, U.S. Army Armament, Munitions and Chemical Command, Dover, NJ 07801
2	ATTN: Technical Library
	Commander, U.S. Army Natick Research, Development and Engineering Center, Natick, MA 01760-5010
1	ATTN: Technical Library
	Commander, U.S. Army Satellite Communications Agency, Fort Monmouth, NJ 07703
1	ATTN: Technical Document Center
	Commander, U.S. Army Tank-Automotive Command, Warren, MI 48397-5000
1	ATTN: AMSTA-ZSK
1	AMSTA-TSL, Technical Library
	Commander, White Sands Missile Range, NM 88002
1	ATTN: STEWS-WS-VT
	President, Airborne, Electronics and Special Warfare Board, Fort Bragg, NC 28307
1	ATTN: Library
	Director, U.S. Army Ballistic Research Laboratory, Aberdeen Proving Ground, MD 21005
1	ATTN: SLCBR-TSB-S (STINFO)
	Commander, Dugway Proving Ground, UT 84022
1	ATTN: Technical Library, Technical Information Division
	Commander, Harry Diamond Laboratories, 2800 Powder Mill Road, Adelphi, MD 20783
1	ATTN: Technical Information Office
	Director, Benet Weapons Laboratory, LCWSL, USA AMCCOM, Watervliet, NY 12189
1	ATTN: AMSMC-LCB-TL
1	AMSMC-LCB-R
1	AMSMC-LCB-RM
1	AMSMC-LCB-RP
	Commander, U.S. Army Foreign Science and Technology Center, 220 7th Street, N.E., Charlottesville, VA 22901-5396
3	ATTN: AIFRTC, Applied Technologies Branch, Gerald Schlesinger
	Commander, U.S. Army Aeromedical Research Unit, P.O. Box 577, Fort Rucker, AL 36360
1	ATTN: Technical Library

No. of Copies	To
	Commander, U.S. Army Aviation Systems Command, Aviation Research and Technology Activity, Aviation Applied Technology Directorate, Fort Eustis, VA 23604-5577
1	ATTN: SAVDL-E-MOS
	U.S. Army Aviation Training Library, Fort Rucker, AL 36360
1	ATTN: Building 5906-5907
	Commander, U.S. Army Agency for Aviation Safety, Fort Rucker, AL 36362
1	ATTN: Technical Library
	Commander, USACDC Air Defense Agency, Fort Bliss, TX 79916
1	ATTN: Technical Library
	Commander, Clarke Engineer School Library, 3202 Nebraska Ave., N, Ft. Leonard Wood, MO 65473-5000
1	ATTN: Library
	Commander, U.S. Army Engineer Waterways Experiment Station, P.O. Box 631, Vicksburg, MS 39180
1	ATTN: Research Center Library
	Commandant, U.S. Army Quartermaster School, Fort Lee, VA 23801
1	ATTN: Quartermaster School Library
	Naval Research Laboratory, Washington, DC 20375
1	ATTN: Code 5830
2	Dr. G. R. Yoder - Code 6384
	Chief of Naval Research, Arlington, VA 22217
1	ATTN: Code 471
1	Edward J. Morrissey, WRDC/MLTE, Wright-Patterson Air Force Base, OH 45433-6523
	Commander, U.S. Air Force Wright Research & Development Center, Wright-Patterson Air Force Base, OH 45433-6523
1	ATTN: WRDC/MLLP, M. Forney, Jr.
1	WRDC/MLBC, Mr. Stanley Schulman
	NASA - Marshall Space Flight Center, MSFC, AL 35812
1	ATTN: Mr. Paul Schuerer/EH01
	U.S. Department of Commerce, National Institute of Standards and Technology, Gaitherburg, MD 20899
1	ATTN: Stephen M. Hsu, Chief, Ceramics Division, Institute for Materials Science and Engineering
1	Committee on Marine Structures, Marine Board, National Research Council, 2101 Constitution Avenue, N.W., Washington, DC 20418
1	Materials Sciences Corporation, Suite 250, 500 Office Center Drive, Fort Washington, PA 19034-3213
1	Charles Stark Draper Laboratory, 68 Albany Street, Cambridge, MA 02139
	Wyman-Gordon Company, Worcester, MA 01601
1	ATTN: Technical Library
	General Dynamics, Convair Aerospace Division P.O. Box 748, Forth Worth, TX 76101
1	ATTN: Mfg. Engineering Technical Library
	Plastics Technical Evaluation Center, PLASTEC, ARDEC Bldg. 355N, Picatinny Arsenal, NJ 07806-5000
1	ATTN: Harry Pebly
1	Department of the Army, Aerostructures Directorate, MS-266, U.S. Army Aviation R&T Activity - AVSCOM, Langley Research Center, Hampton, VA 23665-5225
1	NASA - Langley Research Center, Hampton, VA 23665-5225
1	U.S. Army Propulsion Directorate, NASA Lewis Research Center, 2100 Brookpark Road, Cleveland, OH 44135-3191
1	NASA - Lewis Research Center, 2100 Brookpark Road, Cleveland, OH 44135-3191
	Southwest Research Institute, 6220 Culebra Road, P.O. Drawer 28510, San Antonio, TX 78228-0510
1	ATTN: Bruce L. Morris, P.E.
	Director, U.S. Army Materials Technology Laboratory, Watertown, MA 02172-0001
2	ATTN: SLCMT-TML
4	Authors

U.S. Army Materials Technology Laboratory
Watertown, Massachusetts 02172-0001
EVALUATION OF 8090 AND WELDALITE-049
ALUMINUM-LITHIUM ALLOYS -
Thomas M. Holmes, Ernest S. C. Chin,
Paul J. Huang, and Robert E. Pasternak

Technical Report MTL TR 92-59, September 1992, 34 pp -
illus-tables,

AD ____________

UNCLASSIFIED
UNLIMITED DISTRIBUTION

Key Words

Aluminum-lithium alloys
Mechanical properties
Microstructure

Aluminum-lithium (Al-Li) alloys with their high strength, high stiffness, and low density continue to be of great interest to the aerospace industry. The microstructue, properties and fracture of 8090-T8771 and Weldalite™ 049-T8 Al-Li alloys were studied at MTL in participation with a cooperative round robin sponsored by the Air Force Advanced Aluminum Alloy Test Program. Both 8090 and Weldalite Al-Li alloys demonstrate superior strength to weight ratios compared to the 2519 and 5083 aluminum armor alloys. The 8090 alloy possesses comparable mechanical and ballistic properties to 2519, while providing an 8% reduction in density. The Weldalite has a comparable density to 2519 but demonstrates improvements of over 25% in yield strength, ultimate tensile strength and fracture toughness. Both Al-Li alloys display significantly improved axial fatigue properties over 2519. Under static loading, both materials display mixed modes of transgranular shear, microductility and intersubgranular failure. Under ballistic testing, both alloys display mixed modes of dynamic failure by plugging, spalling and delamination. Whether the goal is to reduce weight or to improve strength, Al-Li alloys offer significant potential for replacing alloys such as 2519 and 5083 as lightweight, high-strength structural armor materials.

U.S. Army Materials Technology Laboratory
Watertown, Massachusetts 02172-0001
EVALUATION OF 8090 AND WELDALITE-049
ALUMINUM-LITHIUM ALLOYS -
Thomas M. Holmes, Ernest S. C. Chin,
Paul J. Huang, and Robert E. Pasternak

Technical Report MTL TR 92-59, September 1992, 34 pp -
illus-tables,

AD ____________

UNCLASSIFIED
UNLIMITED DISTRIBUTION

Key Words

Aluminum-lithium alloys
Mechanical properties
Microstructure

Aluminum-lithium (Al-Li) alloys with their high strength, high stiffness, and low density continue to be of great interest to the aerospace industry. The microstructue, properties and fracture of 8090-T8771 and Weldalite™ 049-T8 Al-Li alloys were studied at MTL in participation with a cooperative round robin sponsored by the Air Force Advanced Aluminum Alloy Test Program. Both 8090 and Weldalite Al-Li alloys demonstrate superior strength to weight ratios compared to the 2519 and 5083 aluminum armor alloys. The 8090 alloy possesses comparable mechanical and ballistic properties to 2519, while providing an 8% reduction in density. The Weldalite has a comparable density to 2519 but demonstrates improvements of over 25% in yield strength, ultimate tensile strength and fracture toughness. Both Al-Li alloys display significantly improved axial fatigue properties over 2519. Under static loading, both materials display mixed modes of transgranular shear, microductility and intersubgranular failure. Under ballistic testing, both alloys display mixed modes of dynamic failure by plugging, spalling and delamination. Whether the goal is to reduce weight or to improve strength, Al-Li alloys offer significant potential for replacing alloys such as 2519 and 5083 as lightweight, high-strength structural armor materials.

U.S. Army Materials Technology Laboratory
Watertown, Massachusetts 02172-0001
EVALUATION OF 8090 AND WELDALITE-049
ALUMINUM-LITHIUM ALLOYS -
Thomas M. Holmes, Ernest S. C. Chin,
Paul J. Huang, and Robert E. Pasternak

Technical Report MTL TR 92-59, September 1992, 34 pp -
illus-tables,

AD ____________

UNCLASSIFIED
UNLIMITED DISTRIBUTION

Key Words

Aluminum-lithium alloys
Mechanical properties
Microstructure

Aluminum-lithium (Al-Li) alloys with their high strength, high stiffness, and low density continue to be of great interest to the aerospace industry. The microstructue, properties and fracture of 8090-T8771 and Weldalite™ 049-T8 Al-Li alloys were studied at MTL in participation with a cooperative round robin sponsored by the Air Force Advanced Aluminum Alloy Test Program. Both 8090 and Weldalite Al-Li alloys demonstrate superior strength to weight ratios compared to the 2519 and 5083 aluminum armor alloys. The 8090 alloy possesses comparable mechanical and ballistic properties to 2519, while providing an 8% reduction in density. The Weldalite has a comparable density to 2519 but demonstrates improvements of over 25% in yield strength, ultimate tensile strength and fracture toughness. Both Al-Li alloys display significantly improved axial fatigue properties over 2519. Under static loading, both materials display mixed modes of transgranular shear, microductility and intersubgranular failure. Under ballistic testing, both alloys display mixed modes of dynamic failure by plugging, spalling and delamination. Whether the goal is to reduce weight or to improve strength, Al-Li alloys offer significant potential for replacing alloys such as 2519 and 5083 as lightweight, high-strength structural armor materials.

U.S. Army Materials Technology Laboratory
Watertown, Massachusetts 02172-0001
EVALUATION OF 8090 AND WELDALITE-049
ALUMINUM-LITHIUM ALLOYS -
Thomas M. Holmes, Ernest S. C. Chin,
Paul J. Huang, and Robert E. Pasternak

Technical Report MTL TR 92-59, September 1992, 34 pp -
illus-tables,

AD ____________

UNCLASSIFIED
UNLIMITED DISTRIBUTION

Key Words

Aluminum-lithium alloys
Mechanical properties
Microstructure

Aluminum-lithium (Al-Li) alloys with their high strength, high stiffness, and low density continue to be of great interest to the aerospace industry. The microstructue, properties and fracture of 8090-T8771 and Weldalite™ 049-T8 Al-Li alloys were studied at MTL in participation with a cooperative round robin sponsored by the Air Force Advanced Aluminum Alloy Test Program. Both 8090 and Weldalite Al-Li alloys demonstrate superior strength to weight ratios compared to the 2519 and 5083 aluminum armor alloys. The 8090 alloy possesses comparable mechanical and ballistic properties to 2519, while providing an 8% reduction in density. The Weldalite has a comparable density to 2519 but demonstrates improvements of over 25% in yield strength, ultimate tensile strength and fracture toughness. Both Al-Li alloys display significantly improved axial fatigue properties over 2519. Under static loading, both materials display mixed modes of transgranular shear, microductility and intersubgranular failure. Under ballistic testing, both alloys display mixed modes of dynamic failure by plugging, spalling and delamination. Whether the goal is to reduce weight or to improve strength, Al-Li alloys offer significant potential for replacing alloys such as 2519 and 5083 as lightweight, high-strength structural armor materials.